

A simplified probing controller for glucose feeding in *Escherichia coli* cultivations

Mats Åkesson* Per Hagander

Department of Automatic Control, Lund Institute of Technology, Lund, Sweden

Abstract A strategy for control of the glucose feed rate in cultivations of *E. coli* is discussed. By making probing pulses in the feed rate it is possible to detect and avoid a characteristic saturation linked to undesirable by-product formation. A simplification of a previous algorithm is presented and analyzed.

1. Introduction

Many proteins are today produced using genetically modified microorganisms. Recombinant DNA technology makes it possible to insert DNA coding for a foreign protein into a host organism, thereby creating a “cell factory” for the protein. The bacterium *Escherichia coli* is a common host. It can be grown to high cell densities but a problem is the accumulation of the metabolic by-product acetate, which tends to inhibit growth and production [6, 8].

Formation of acetate occurs under anaerobic conditions but also under aerobic conditions in situations with excess carbon source. Accumulation of acetate can be reduced by manipulation of strains, media, and cultivation conditions. In fed-batch cultures the feed rate of the carbon source, typically glucose, can be manipulated to restrict acetate formation. A number of feeding strategies have been developed [7, 11], however, most of them require considerable process knowledge to work well, and the implementation often relies on specialized and expensive sensors.

In [1, 2] we presented a probing feeding strategy that requires a minimum of process knowledge and is implemented using standard sensors. Lab-scale experiments under various operating conditions have shown that the method reproducibly works well. In this paper we present a simplified controller which yields facilitated analysis, and better performance.

2. Process Description

E. coli bacteria are cultivated in a stirred bioreactor with a liquid medium containing cells and substrates, see Figure 1. Air is sparged into the liquid in

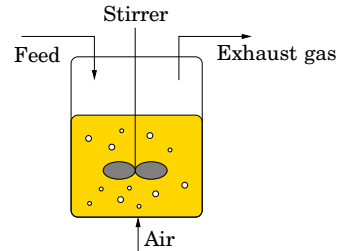


Figure 1 A stirred bioreactor with incoming feed flow.

order to supply the culture with oxygen. Well-mixed conditions are obtained through agitation with a stirrer and the stirrer speed is also used to adjust the oxygen transfer rate. Control loops for temperature, pH, and dissolved oxygen ensure that suitable operating conditions are maintained. After an initial batch phase, the main substrate glucose is fed at a growth-limiting rate. In this way, the feed rate can be used to manipulate the glucose uptake and the growth rate. Typically, the process is divided into a growth phase where the cell mass is increased, and a production phase where production of the recombinant protein is induced.

We will now briefly recapitulate a model for an aerobic fed-batch cultivation of *E. coli*. Particular attention is paid to the dynamic relation between dissolved oxygen and glucose feed rate. For details on parameters and metabolic expressions see [1].

2.1 Metabolic Relations

The cell metabolism is described by the specific rates of growth μ , glucose uptake q_g , oxygen uptake q_o , and net production of acetate q_a . The metabolic expressions used are largely similar to the ones presented in [12]. Glucose provides energy and raw material for cell growth. The specific glucose uptake, q_g , is taken to be of Monod type

$$q_g(G) = q_g^{max} G / (k_s + G)$$

which describes a smoothly saturating glucose uptake. Oxygen is used to metabolize the glucose, and the specific oxygen uptake q_o depends on q_g .

* Corresponding author. Present address: Biotecnol SA, Taguspark, Oeiras, Portugal. e-mail: ma@biotecnol.com

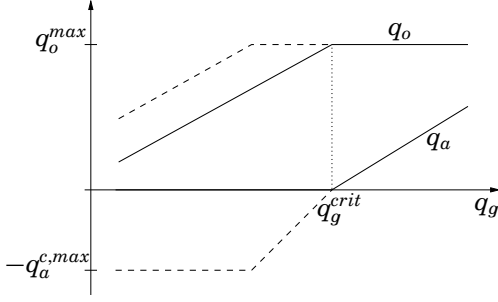


Figure 2 Relations between specific rates of glucose uptake, q_g , oxygen uptake, q_o , and net acetate production, q_a . Dashed lines show potential acetate consumption and its effect on q_o when acetate is present in the media.

Formation of acetate under aerobic conditions typically occurs when q_g exceeds a critical value q_g^{crit} . It has also been observed that q_o reaches an apparent maximum q_o^{max} at the onset of acetate formation [4, 9] as illustrated by the solid lines in Figure 2. Acetate present in the medium may also be consumed and used for growth. Its uptake mechanism is likewise modeled to follow Monod kinetics

$$q_a^{c,pot} = q_a^{c,max} A / (k_a + A)$$

However, as the consumption requires oxygen and glucose is the preferred substrate, it is limited both by the available oxidative capacity and the uptake mechanism. The dashed lines in Figure 2 outlines the maximum potential acetate consumption and the resulting effect on q_o . The specific growth rate μ increases with the glucose uptake but with a decreased yield above q_g^{crit} . Consumption of acetate also contributes to the cell growth.

2.2 Bioreactor Model

Component-wise mass balances for the bioreactor give the following equations

$$\begin{aligned} \frac{dV}{dt} &= F \\ \frac{d(VX)}{dt} &= \mu(G, A) \cdot VX \\ \frac{d(VG)}{dt} &= FG_{in} - q_g(G) \cdot VX \\ \frac{d(VA)}{dt} &= q_a(G, A) \cdot VX \\ \frac{d(VC_o)}{dt} &= K_L \alpha(N) \cdot V(C_o^* - C_o) - q_o(G, A) \cdot VX \end{aligned}$$

where V , X , G , A , C_o are the liquid volume, the cell concentration, the glucose concentration, the acetate concentration, and the dissolved oxygen concentration, respectively. Further, F , G_{in} , C_o^* denote the feed rate, the glucose concentration in the feed, and the dissolved oxygen concentration in equilibrium with the oxygen in gas bubbles. The volumetric

oxygen transfer coefficient, $K_L \alpha$, increases with the stirrer speed N but is also affected by factors like viscosity, foaming, and anti-foam chemicals.

When the measurement of dissolved oxygen is used for control, it is also important to consider the dynamics in the dissolved oxygen probe. In practice, most sensors measure the dissolved oxygen tension which is related to the dissolved oxygen concentration through Henry's law $O = H \cdot C_o$. The probe is here modeled as a first-order system

$$T_p \frac{dO_p}{dt} + O_p = O \quad (1)$$

2.3 Linearized Model

Over short periods of time, V and X are approximately constant. The dynamics for deviations in glucose uptake and dissolved oxygen due to changes in F may then be approximated by the linear equations

$$T_g \frac{d\Delta q_g}{dt} + \Delta q_g = K_g \Delta F \quad (2)$$

$$T_o \frac{d\Delta O}{dt} + \Delta O = K_o \Delta q_g \quad (3)$$

where the gains and the time constants vary significantly during a cultivation. Typically, T_g and T_o decrease with increasing biomass. Below the respiratory saturation, equations (2) and (3) together with the model for the sensor (1) give a third-order linear model relating ΔF and ΔO_p . In [1] it is shown that the stationary gain can be rewritten as

$$K = K_g K_o = -(O^* - O_{sp}) / ((1 + \alpha)F) \quad (4)$$

where α normally is close to 0 but may approach 1 for high acetate concentrations or low glucose uptakes.

2.4 Control Problem

It is often desirable to keep F high since this will give faster growth and a minimized process time, thereby improving productivity. However, to avoid accumulation of acetate the glucose feed rate F should be kept low so that overflow metabolism is avoided and aerobic conditions maintained. In other words, the resulting specific glucose uptake q_g should be less than q_g^{crit} and the oxygen consumption less than the maximum achievable oxygen transfer in the reactor. The handling of the limited oxygen transfer was described in [1] and we will here concentrate on avoiding overflow metabolism. A major challenge is the time-varying and uncertain nature of the process. For instance, q_g^{crit} is often poorly known and it may also change during a cultivation, especially during production of a recombinant protein [3, 10].

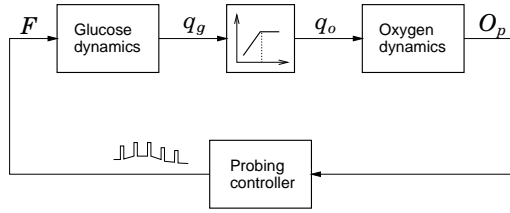


Figure 3 The probing control strategy. By making probing pulses in F it is possible to determine if q_g is above or below q_g^{crit} from the response in O_p .

3. A Probing Control Strategy

The key idea of the probing feeding controller is to exploit the characteristic saturation in the respiration that occurs when q_g exceeds q_g^{crit} and acetate formation starts. The saturation can be detected by superimposing probing pulses in F that are long enough to be seen through the system dynamics. As long as q_g is below q_g^{crit} , the pulses give rise to responses in the dissolved oxygen signal O_p . However, when q_g is above q_g^{crit} , q_o is saturated and no response is seen. In this way it is possible to determine if q_g is above or below q_g^{crit} without knowledge of the actual value [3]. This information is then used to adjust F to achieve feeding at q_g^{crit} , see Figure 3. The probing controller can be viewed as an extremum controller, see [5], controlling the process to a saturation instead of an optimum.

3.1 A Simplified Feedback Algorithm

The previous implementation of the algorithm [1, 2] made use of both up and down pulses in a switching scheme depending on the pulse responses. The down pulses are here omitted while maintaining, and even improving, performance. The simplification also makes implementation and analysis easier.

At each cycle of the algorithm, a pulse is given to get information. If the amplitude of the response in dissolved oxygen $|O_{pulse}|$ exceeds a threshold level O_{reac} , the feed rate is increased as

$$\Delta F(k) = \kappa \cdot F(k) |O_{pulse}(k)| / (O^* - O_{sp}) \quad (5)$$

Otherwise, if $|O_{pulse}| < O_{reac}$, it is concluded that q_g exceeds q_g^{crit} and F is decreased with a fixed amount chosen to be equal to the pulse size F_{pulse} . An example is shown in Figure 4 where also some of the algorithm parameters are defined.

To ensure that O_p starts from the same level, O_{sp} , at each pulse, it is regulated by manipulation of the stirrer speed. During the feed pulses, however, the stirrer speed is fixed in order not to interfere with the detection algorithm. If disturbances cause O_p to deviate from the set-point at the time for a pulse, a safety net delays the pulse to avoid erroneous interpretations of the pulse response.

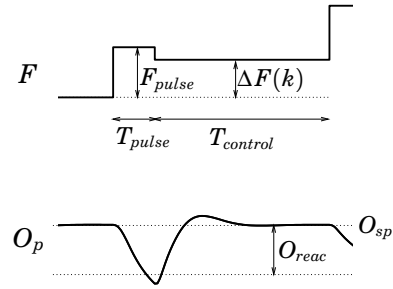


Figure 4 Example of a cycle in the algorithm. During the time $T_{control}$ between two pulses, O_p is regulated by a controller manipulating the stirrer speed.

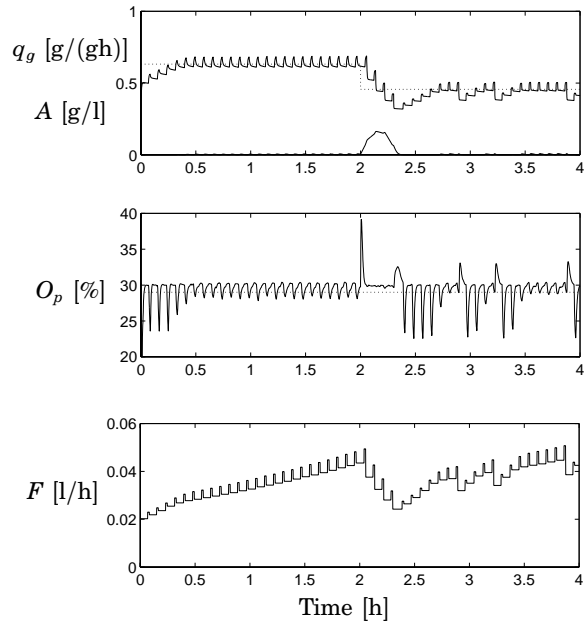


Figure 5 Simulation with $\kappa = 1$ where the initial feed rate is chosen too low. After two hours q_g^{crit} is changed. The dotted lines indicate the critical glucose uptake, q_g^{crit} , and the reaction level O_{reac} . The probing controller achieves feeding at q_g^{crit} without prior information of the value and in spite of the change.

3.2 Simulation Example

A simulation of the simplified algorithm is shown in Figure 5 where the initial feed rate after a batch phase gives a specific glucose uptake q_g below q_g^{crit} . The controller increases F until q_g^{crit} is reached and q_g is then kept approximately constant as desired. After 2 hours the value of q_g^{crit} is decreased, and as can be seen the algorithm is able to detect and adjust the feed accordingly. The undershoot is due to reconsumption of the acetate produced when q_g temporarily exceeds q_g^{crit} . The accompanying oxygen consumption gives $q_o = q_o^{max}$ even though $q_g < q_g^{crit}$ and hence F is decreased as no oxygen responses can be seen. This example illustrates the ability to achieve feeding at q_g^{crit} without *a priori* information and in spite of changes that may occur in the process.

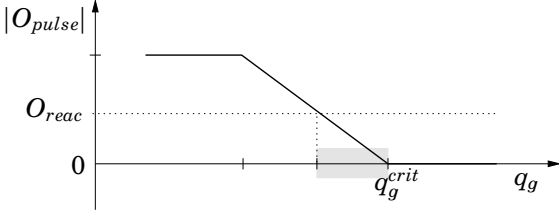


Figure 6 Amplitude of the pulse responses in dissolved oxygen $|O_{pulse}|$ as a function of q_g . The shaded area indicates the region where $|O_{pulse}| < O_{reac}$ and $q_g < q_g^{crit}$.

3.3 Guidelines for Tuning

In the next section, we show how to choose the “controller gain” κ in (5). Tuning rules for the other parameters were derived in [1] based on the linearized process model. The only required information is an upper bound for the lumped time constant T_{max} in the relation between F and O_p together with the noise level in O_p . These quantities are mainly equipment related and do not depend critically on a particular strain or product.

4. Stability Analysis

The closed-loop system is non-linear and contains elements of continuous-time as well as discrete-time nature and a complete analysis is therefore difficult. However, by considering it as a sampled-data system it is possible to derive a sufficient condition for convergence to a region below but close to q_g^{crit} .

4.1 Characterization of Oxygen Responses

When checking the oxygen response O_{pulse} to pulses in the feed rate F , the pulse length T_{pulse} is chosen equal to the estimated process time constant T_{max} as recommended in [1]. This is long compared to the glucose dynamics, and we may then assume $q_g^{pulse} \approx K_g \cdot F_{pulse}$. Consider the response to a pulse starting at q_g . Obviously, if q_g is above q_g^{crit} no response will be seen. For q_g far below q_g^{crit} , the amplitude of O_{pulse} is given by the linearized model as $|O_{pulse}| = \beta |K_o| \cdot q_g^{pulse}$ where $0.63 < \beta < 1$ accounts for the dynamics and the finite pulse time. As q_g approaches to q_g^{crit} , the saturation in q_o will cause a reduced response, and only the part of the pulse that is below q_g^{crit} will contribute to O_{pulse} . This is summarized in the piecewise linear function

$$|O_{pulse}| = \begin{cases} 0, & \text{if } q_g > q_g^{crit} \\ \beta |K_o| q_g^{pulse}, & \text{if } q_g < q_g^{crit} - q_g^{pulse} \\ \beta |K_o| (q_g^{crit} - q_g), & \text{otherwise} \end{cases} \quad (6)$$

shown in Figure 6. The shaded area indicates where $|O_{pulse}| < O_{reac}$ even though $q_g < q_g^{crit}$. As O_{pulse} also depends on β , which changes during a cultivation, the width of the shaded region will change.

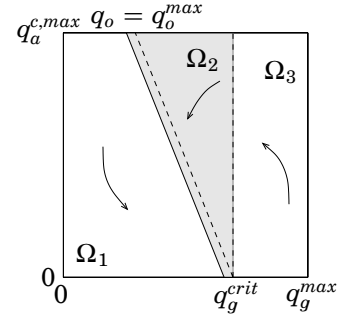


Figure 7 Regions in the plane $(q_g, q_a^{c.pot})$. The shaded region Ω_2 indicates where $|O_{pulse}| < O_{reac}$ even though $q_g < q_g^{crit}$. The arrows indicate qualitative trajectories of the closed-loop system.

4.2 Effects from Acetate Consumption

If $q_g < q_g^{crit}$, the cells may consume acetate present in the media with a concomitant consumption of oxygen. It is important to include this in the analysis, as the specific oxygen uptake q_o may be saturated even if $q_g < q_g^{crit}$. In Figure 7 we introduce the plane $(q_g, q_a^{c.pot})$ where $q_a^{c.pot} = q_a^{c.max} A / (k_a + A)$. To the right of q_g^{crit} acetate is produced, and to the left acetate may be consumed. In the region between the two dashed lines, we have $q_o = q_o^{max}$ and hence the acetate consumption is there limited by the available respiratory capacity. To the left of this region the acetate consumption is limited only by the uptake mechanism and $q_o < q_o^{max}$. As before, the shaded region indicates where $|O_{pulse}| < O_{reac}$ and $q_g < q_g^{crit}$. We will denote this region Ω_2 , and the regions to its left and right, Ω_1 and Ω_3 , respectively.

4.3 Closed-loop System

The controller connected to the process is now treated as a sampled-data system with sampling period $T_{pulse} + T_{control}$ and we consider the possible trajectories in the plane $(q_g, q_a^{c.pot})$. Acetate is consumed to the left of the line $q_g = q_g^{crit}$. Hence A and $q_a^{c.pot}$ will decrease in this region. Conversely, when $q_g > q_g^{crit}$, acetate is produced and $q_a^{c.pot}$ increases. In the q_g -direction the controller directly affects the process. The choice of the sampling interval assure that the glucose dynamics can be neglected and thus

$$\Delta q_g(k) = q_g(k+1) - q_g(k) = K_g \cdot \Delta F(k) - \varepsilon \quad (7)$$

where ε accounts for the influence from the changing cell mass VX . In Ω_1 , we have $|O_{pulse}(k)| > O_{reac}$. Hence $\Delta F(k) > 0$ and $q_g(k)$ will increase. Conversely, in Ω_2 and Ω_3 , $\Delta F(k) < 0$ and $q_g(k)$ will decrease until these regions are escaped to the left. Qualitative trajectories, when neglecting the drift from the ε -term, are indicated by the arrows in Figure 7. Note, however, that the discussion below holds even if ε is larger than zero.

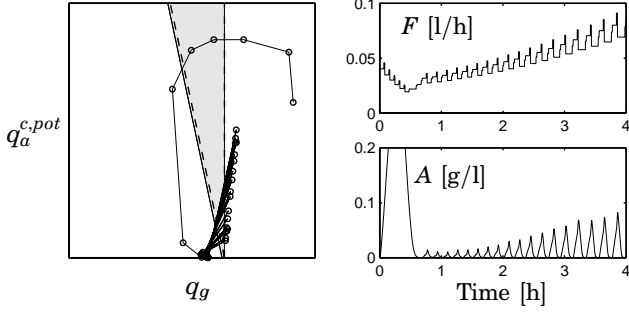


Figure 8 Oscillatory behavior when the feed increments are too large, $\kappa = 2.5$. Left: Trajectory of the sampled-data system in the plane $(q_g, q_a^{c.pot})$. Right: Feed rate F and acetate concentration A .

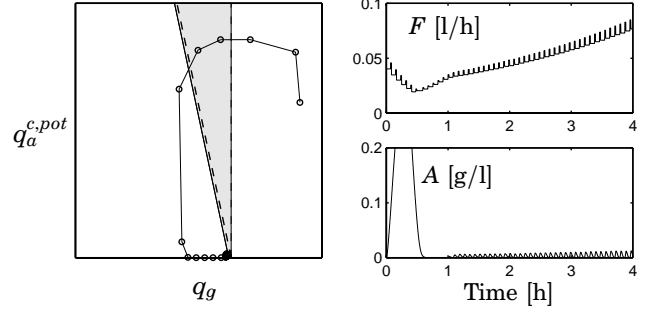


Figure 9 Convergent behavior when $\kappa = 1$. Left: Trajectory of the sampled-data system in the plane $(q_g, q_a^{c.pot})$. Right: Feed rate F , acetate concentration A .

We see that if $\Delta q_g(k)$ is too large, we cannot exclude “limit cycles” where the process is oscillating between Ω_1 and Ω_3 . An example of this is shown in Figure 8 which shows a simulation with $\kappa = 2.5$. The key to avoiding oscillatory behavior is to ensure that $\Delta q_g(k)$ is smaller than the shortest distance from Ω_1 to the line q_g^{crit} . Then all trajectories starting in Ω_1 or Ω_2 will remain to the left of q_g^{crit} . Furthermore, as all trajectories to the left of q_g^{crit} tend downwards, we can conclude that there exist attractive invariant sets M in the lower right part of this region. As all trajectories starting to the right of q_g^{crit} will end up to its left, any M is globally attractive.

4.4 A Sufficient Condition for Stability

The condition that $\Delta q_g(k)$ should be smaller than the shortest distance from Ω_1 to the line q_g^{crit} will now be translated to a sufficient bound on κ . For any $|O_{pulse}| > 0$, we know from (6) that $|O_{pulse}/K_o| < q_g^{crit} - q_g$. Now, by using $\varepsilon \geq 0$ in (7) together with (5) and (4) we get

$$\Delta q_g(k) \leq K_g \Delta F(k) \leq \frac{\kappa |O_{pulse}(k)|}{(1 + \alpha) |K_o|} \leq \kappa (q_g^{crit} - q_g) \quad (8)$$

Hence, stability is ensured if we choose $\kappa \leq 1$. A simulation with $\kappa = 1$ is shown in Figure 9. As expected the system converges, without oscillations, to the desired region to the left of q_g^{crit} .

5. Setpoint and Integral Action

In the simulation shown in Figure 9, the system seems to converge to a well-controlled “stationary” situation where the oxygen response is larger than O_{reac} . This is not always so, even if $\kappa \leq 1$, see for instance the later part of the simulation in Figure 5. A linear analysis reveals conditions for the existence of a fix point in the “proportional band” below q_g^{crit} , and suggests the introduction of a set-point and integral action to enhance the convergence.

5.1 Convergence to Stationarity

Assume that $A \approx 0$ and that any acetate resulting from a probing pulse is consumed before the next pulse. For convenience, introduce $y \equiv |O_{pulse}|$. Inside the proportional band defined by (6), y is given by

$$y(k) = \beta |K_o| \cdot (q_g^{crit} - q_g) \quad (9)$$

From the process equation (7) we can obtain

$$y(k+1) = y(k) - \beta |K_o| K_g \Delta F(k) + \beta |K_o| \varepsilon \quad (10)$$

Using (5) and (4) we finally get

$$y(k+1) = \{1 - \beta \kappa / (1 + \alpha)\} y(k) + \beta |K_o| \varepsilon \quad (11)$$

and when $0 < \kappa < 2(1 + \alpha)/\beta$, we see that $y(k)$ converges to

$$y^* = (1 + \alpha) |K_o| \varepsilon / \kappa \quad (12)$$

Hence, if the drift from ε is such that $y^* > O_{reac}$, the process will converge to a stationary point below q_g^{crit} . However, if O_{reac} is too large or ε is too small the controller will change between increments and decrements as in the right part of Figure 5.

5.2 Introducing a Setpoint and Integral Action

By introducing a set-point y_r in the control law

$$\Delta F(k) = \kappa \cdot \frac{y(k) - y_r}{O^* - O_{sp}} \cdot F \quad (13)$$

the fix point y^* is shifted to

$$y^* = (1 + \alpha) |K_o| \varepsilon / \kappa + y_r$$

Hence, by choosing $y_r > O_{reac}$ we get $y^* > O_{reac}$, even if $\varepsilon = 0$. If y_r is too large, y saturates and the maximum control signal gives a q_g below the proportional band. A better solution is to introduce integral action

$$\Delta F(k) = \left(\kappa \cdot (y(k) - y_r) + \kappa_i \sum_{j=0}^k (y(j) - y_r) \right) \frac{F}{O^* - O_{sp}}$$

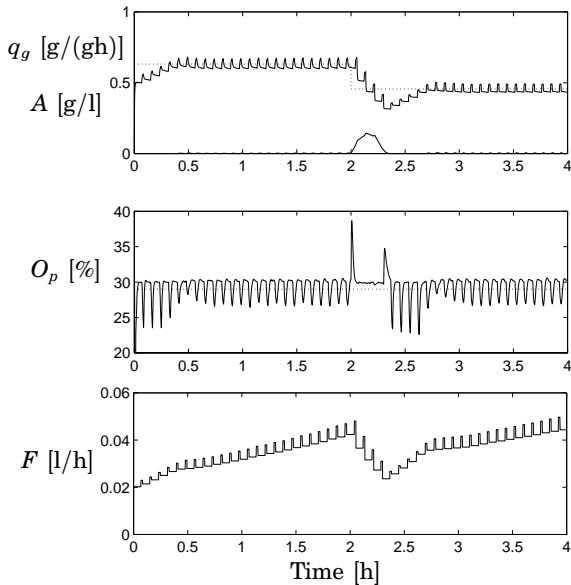


Figure 10 Simulation with PI controller ($\kappa = 0.96$, $\kappa_i = 0.64$) where q_g^{crit} is changed after two hours. The dotted lines indicate the critical glucose uptake, q_g^{crit} , and the reaction level O_{reac} . Feeding at q_g^{crit} is achieved and after the transients the amplitude of the oxygen responses reach the set-point $y_r = 3$ which eliminates the “oscillations” seen in Figure 5.

which gives $y^* = y_r$ if the stability condition

$$\kappa > 0, \kappa_i > 0, 2\kappa + \kappa_i < 4(1 + \alpha)/\beta \quad (14)$$

is fulfilled. Thus, convergence is assured by choosing y_r in the proportional band and larger than O_{reac} .

Outside the proportional band the integral is recalculated so that the stability condition induced by (8) is fulfilled. In this way the global stability property is maintained and wind-up effects are avoided. Figure 10 shows a simulation with PI control ($\kappa = 0.96$, $\kappa_i = 0.64$) using $y_r = 3$. The setting is the same as in Figure 5 and again feeding at q_g^{crit} is achieved. However, after the transients the amplitude of the oxygen responses reaches the set-point and this eliminates the “oscillations” seen in Figure 5. The fluctuations seen are due to noise added in the simulation.

6. Conclusions

In cultivations of *E. coli* it is important to avoid accumulation of the by-product acetate, which is produced when the specific glucose uptake q_g exceeds a critical value q_g^{crit} . We have discussed an approach for control of glucose feeding based on a superimposed probing signal in the feed rate. It can be implemented with standard instrumentation and enables control of q_g at an unknown and time-varying q_g^{crit} . The primary contribution of this paper is a simplified algorithm and a stability analysis that gives a sufficient condition for convergence.

Acknowledgments

Financial support from Pharmacia & Upjohn, the Swedish National Board for Industrial and Technical Development (project 1N11-97-09517), and the Alf Åkerman foundation is gratefully acknowledged.

7. References

- [1] M. Åkesson. “Probing control of glucose feeding in *Escherichia coli* cultivations.” PhD Thesis ISRN LUTFD2/TFRT-1057-SE, Department of Automatic Control, Lund Institute of Technology, Sweden, December 1999.
- [2] M. Åkesson, P. Hagander, and J. P. Axelsson. “A probing feeding strategy for *Escherichia coli* cultures.” *Biotechnology Techniques*, **13**, pp. 523–528, 1999.
- [3] M. Åkesson, E. Nordberg Karlsson, P. Hagander, J. P. Axelsson, and A. Tocaj. “On-line detection of acetate formation in *Escherichia coli* cultures using dissolved oxygen responses to feed transients.” *Biotechnology and Bioengineering*, **64**, pp. 590–598, 1999.
- [4] K. Andersen and K. von Meyenburg. “Are growth rates of *Escherichia coli* in batch cultures limited by respiration?” *Journal of Bacteriology*, **144**, pp. 114–123, 1980.
- [5] K. J. Åström and B. Wittenmark. *Adaptive Control*. Addison-Wesley, Reading, Massachusetts, second edition, 1995.
- [6] E. Bech Jensen and S. Carlsen. “Production of recombinant human growth hormone in *Escherichia coli*: expression of different precursors and physiological effects of glucose, acetate and salts.” *Biotechnology and Bioengineering*, **36**, pp. 1–11, 1990.
- [7] S. Y. Lee. “High cell-density culture of *Escherichia coli*.” *Trends in Biotechnology*, **14**, pp. 98–105, 1996.
- [8] G. W. Luli and W. R. Strohl. “Comparison of growth, acetate production, and acetate inhibition of *Escherichia coli* strains in batch and fed-batch fermentations.” *Applied and Environmental Microbiology*, **56**, pp. 1004–1011, 1990.
- [9] T. Paalme, R. Elken, A. Kahru, K. Vanatalu, and R. Vilu. “The growth rate control in *Escherichia coli* at near to maximum growth rates: the A-stat approach.” *Antonie van Leeuwenhoek*, **71**, pp. 217–230, 1997.
- [10] J. Qiu, J. R. Swartz, and G. Georgiou. “Expression of active human tissue-type plasminogen activator in *Escherichia coli*.” *Applied and Environmental Microbiology*, **64**, pp. 4891–4896, 1998.
- [11] D. Riesenberger and R. Guthke. “High-cell-density cultivation of microorganisms.” *Applied Microbiology and Biotechnology*, **51**, pp. 422–430, 1999.
- [12] B. Xu, M. Jahic, and S.-O. Enfors. “Modeling of overflow metabolism in batch and fed-batch cultures of *Escherichia coli*.” *Biotechnology Progress*, **15**, pp. 81–90, 1999.